ACS APPLIED MATERIALS & INTERFACES

www.acsami.org
Research Article

Free-Form Liquid Crystal Elastomers via Embedded 4D Printing

Luke McDougall, Jeremy Herman, Emily Huntley, Samuel Leguizamon, Adam Cook, Timothy White, Bryan Kaehr,* and Devin J. Roach*

Cite This: ACS Appl. Mater. Interfaces 2023, 15, 58897−58904
Read Online

ABSTRACT: Liquid crystal elastomers (LCEs) are a class of active materials that can generate rapid, reversible mechanical actuation in response to external stimuli. Fabrication methods for LCEs have remained a topic of intense research interest in recent years. One promising approach, termed 4D printing, combines the advantages of 3D printing with responsive materials, such as LCEs, to generate smart structures that not only possess user-defined static shapes but also can change their shape over time. To date, 4D-printed LCE structures have been limited to flat objects, restricting shape complexity and associated actuation for smart structure applications. In this work, we report the development of embedded 4D printing to extrude hydrophobic LCE ink into an aqueous, thixotropic gel matrix to produce free-standing, free-form 3D architectures without sacrificing the mechanical actuation properties. The ability to 4D print complex, free-standing 3D LCE architectures opens new avenues for the design and development of functional and responsive systems, such as reconfigurable metamaterials, soft robotics, or biomedical devices.

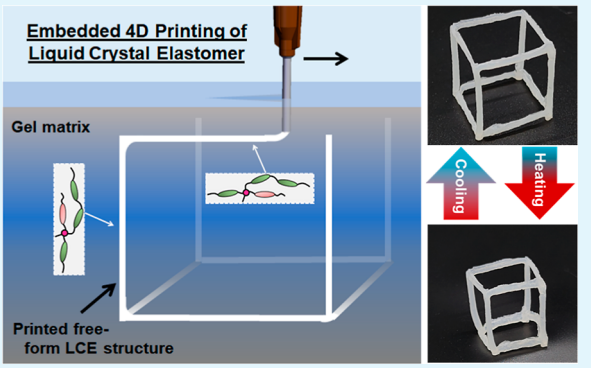

KEYWORDS: *liquid crystal elastomers, embedded printing, 4D printing, free form printing, soft robots, soft mechanics*

1. INTRODUCTION

Additive manufacturing (AM), or 3D printing, has had a vast impact on industries, such as aerospace, construction, and defense. AM is most well known for on-demand fabrication of geometrically complex 3D shapes, some of which are impossible to create by using traditional manufacturing techniques. Meanwhile, advances in stimulus-responsive materials such as hydrogels, shape memory polymers, magneto-active materials, and liquid crystal elastomers (LCEs) have demonstrated unique promise for the fabrication of smart, responsive structures that have found widespread applications in biomedical devices,[1−4] soft robots,[5−8] and deployable structures.[9−13] When 3D-printed, smart materials can transform as a function of time, leading to a new paradigm of printing called 4D printing.[14]

LCEs have stood out as a particularly promising class of smart material for 4D printing as a result of their rapid, reversible mechanical actuation in response to light,[15−17] temperature,[18,19] magnetic fields,[20,21] or biological signals.[22] These large mechanical actuations result from nematic-to-isotropic phase transitions, which cause rotation of the LCE polymer backbone, also known as mesogens. While LCE alignment strategies traditionally rely on mechanical stretching,[23,24] light,[9] or magnetic fields,[25] recent studies have explored the coupling of 3D printing processes and LCE alignment.[26,27] For example, during direct ink write (DIW) 3D printing, LCE mesogens are aligned by the shear forces exhibited on the LCE ink during extrusion through the DIW nozzle.[26,28] This approach has enabled facile fabrication of a myriad of unique geometries, such as conical, lattice, or tensegrity structures for shape-changing assemblies. While DIW can be used for 4D printing of LCE-driven shape-changing structures, only planar 2D architectures can be generated, significantly limiting their applications to in-plane actuation or simple bending shape transformations.

One approach for fabricating nonplanar LCE-based soft actuators is by printing LCE between rigid support structures.[29] This is accomplished using in situ laser-curing during DIW 3D printing which locks LCE mesogen alignment while LCE fibers are printed between rigid supports. Still, this approach requires multiple printing methods to generate a single free-standing structure, and the use of external supports to maintain the desired alignment and geometry of the structure adds complexity to the printing process, which can compromise the inherent LCE properties. Digital light processing (DLP) is another 3D printing technique which has demonstrated significant promise in fabricating geometrically complex 3D LCE structures.[30−32] Nonetheless, these

Received: October 4, 2023
Revised: December 1, 2023
Accepted: December 1, 2023
Published: December 12, 2023

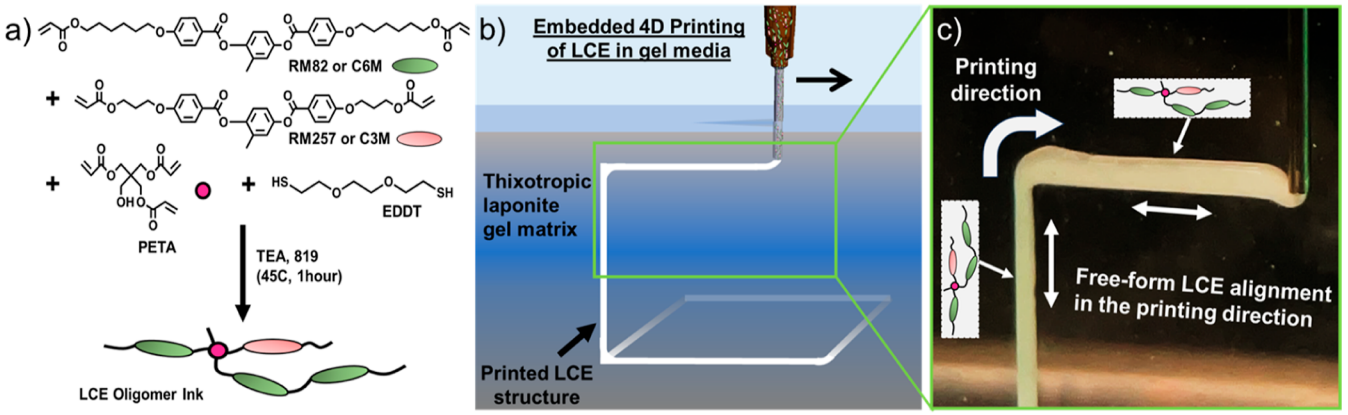

Figure 1. Approach for the embedded 4D printing of LCE in a thixotropic gel matrix. (a) Chemical formulation of the LCE ink used for embedded DIW printing. (b) Schematic showing the embedded DIW printing of an LCE ink into a laponite-based thixotropic gel matrix. (c) Image of LCE printing into the gel matrix, retaining its 3D shape and achieving free-form LCE mesogen alignment.

works require additional programing steps after printing to achieve LCE alignment. Some works have demonstrated LCE alignment during DLP printing, however, they are limited to magnetic field alignment which currently requires large fields (e.g., 500 mT)[33] or surface alignment leading to substantial printing time (e.g., minutes per layer).[34] Therefore, printing complex 3D LCE structures that do not require rigid supports or significant printing time remains a challenge.

Multiphoton lithography (MPL)—a direct laser writing, micro-/nanoscale 3D-printing technique—has been used to print stimulus-responsive actuators including hydrogels[35,36] and LCEs.[37,38] Although shape-complexity is readily achieved using this technique, overall structure dimensions are limited to the microscale, and mesogenic director alignment is restricted to a simple surface pattern (e.g., rubbing angle[39]) or requires a specialized laser/electrode configuration.[37]

Another promising method for printing structurally complex 3D architectures is via embedded printing where materials that are not self-supporting are extruded into a liquid or gel matrix.[40,41] Embedded printing is a method pioneered in biomedical science for the fabrication of cell-based organisms and organ scaffolds.[42−44] Embedded printing of smart, shape-changing materials, here termed embedded 4D printing, has seen limited investigation in the literature. To date, embedded 4D printing has been used to fabricate structures which can change their shape using shape memory polymers (SMP)[45,46] and simple, bilayer hydrogels.[47,48] Nonetheless, SMPs can only achieve one-way shape transformation before requiring reprogramming while hydrogel-based actuation is slow, requiring up to multiple days for large structures.[49] Some researchers have extruded LCE into the liquid matrix to reduce die-swell during extrusion for high-fidelity printed lines[50] or to provide a catalyst for immediate curing of the LCE ink.[51] However, these methods do not use a matrix with a suitable viscosity to print free-form 3D architectures or require human intervention for the LCE mesogen alignment and shape programming. Therefore, generating complex, free-form 3D structures that can provide rapid and reversible shape transformations directly after printing remains a challenge.

In this article, we present a fabrication approach for free-standing, structurally complex 3D LCE structures using embedded 4D printing. The use of a 96 wt % water gel medium offers a perfect candidate for providing structural support for the hydrophobic LCE ink during embedded 4D printing. Furthermore, the addition of a trifunctional acrylate to the traditional LCE ink provides the necessary cross-linking density and resulting mechanical properties required to generate 3D, free-standing LCE structures after removal from the gel, without the need for support structure. The shape changing properties of the LCE were characterized, demonstrating no change in mechanical actuation from traditional methodologies. By embedded 4D printing of LCE ink into a gel medium and increasing cross-link density, it becomes possible to create intricate 3D structures with precise alignment and geometry, while still maintaining the desirable properties of LCE. The elimination of external supports simplifies the printing process, reduces production time, and enhances the mechanical performance of the resulting LCE structures. The ability to 4D print complex 3D LCE structures without the need for supports opens new avenues for the design and development of functional and responsive systems, such as soft robotics, energy harvesters, or biomedical devices.

2. RESULTS AND DISCUSSION

2.1. Embedded 4D Printing of LCEs. Free-form LCE structures were fabricated by using embedded 4D printing to generate novel 3D to 3D shape transformations. The chemical composition of the LCE ink, shown in Figure 1a, was developed using approaches which have been thoroughly investigated in previous works[9,28,29,52] detailing the rheological properties of the LCE ink which are favorable for DIW printing. Importantly, by using a 75/25 wt % ratio of the C6M (RM82) and C3M (RM257) monomers the LCE ink was more readily printable at room temperature conditions.[28] The rheological properties of the LCE ink used in this study can be found in Section S1 of the Supporting Information. In this study, the matrix material used for embedded printing comprised water and laponite to create a thixotropic solution which remains stable for many days.[53] Many considerations were made when selecting the laponite gel matrix material. First, the gel must assist with the shape fixity of the LCE ink. The LCE ink is very hydrophobic, making the water-based laponite gel a perfect candidate for embedded printing of LCE. Second, as noted in multiple studies focusing on embedded 3D printing, the matrix material must be able to recover its shape for printing of future layers. Viscoelastic characteristics of the laponite gel matrix were studied and can be found in Section S2 of the Supporting Information showing that the matrix

https://doi.org/10.1021/acsami.3c14783
ACS Appl. Mater. Interfaces 2023, 15, 58897−58904

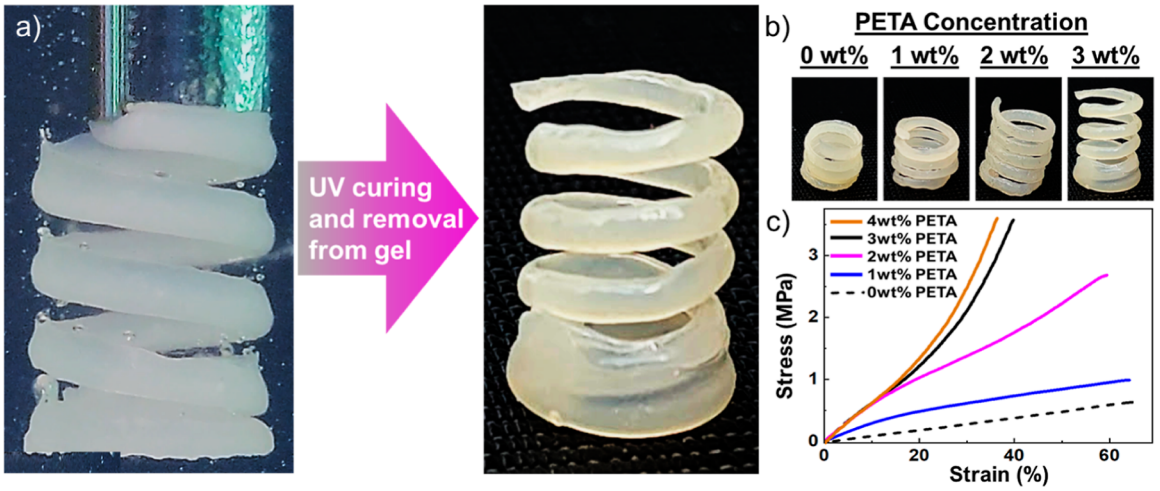

Figure 2. Addition of PETA creates an LCE ink that can generate free-standing structures after embedded printing. (a) In contrast to the LCE ink without PETA, the LCE with PETA can sustain its 3D shape after removal from the gel matrix. (b) Printed objects showing the effect of increased PETA concentration on the ability to generate self-supporting LCE architectures. (c) Mechanical properties of printed LCE with varying concentrations of PETA which exhibit a substantial increase in modulus.

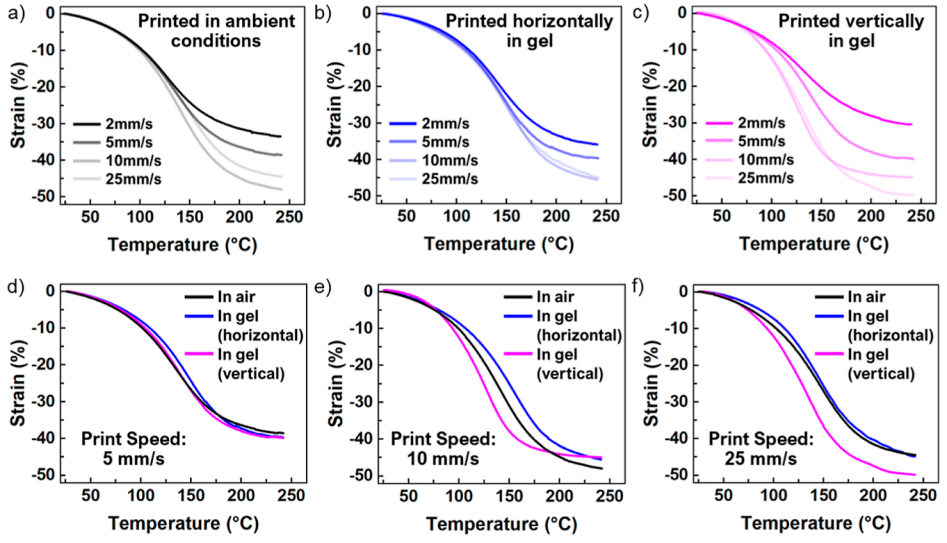

Figure 3. Characterization of the LCE mechanical actuation in response to temperature after being printed (a) in ambient conditions, outside of the gel matrix, (b) horizontally in the gel matrix, and (c) vertically in the gel matrix. (d) Characterization of the LCE mechanical actuation in response to temperature when printed at (d) 5 mm/s, (e) 10 mm/s, and (f) 25 mm/s.

exhibits viscoplastic behavior with rapid shape recovery times. Lastly, the gel must be easily processable, enabling washing out of the LCE structures after printing. Here, the water-based gel matrix enabled the simple washing of the LCE structures using water. Figure 1b provides a schematic illustration of the approach for the embedded 4D printing of LCE structures. Here, LCE ink was extruded into a thixotropic laponite gel matrix which provided structural support to generate unique 3D architectures. Figure 1c shows an image of the LCE ink being extruded into the gel matrix and retaining its shape as the print nozzle moves in 3D space. Complex architectures could be printed using custom toolpath generation software. A video of the printing process for a complex 3D architecture and images of the printing process can be found in Section S3 of the Supporting Information.

2.2. Self-Supporting 3D LCE Structures. After printing in the gel matrix, the LCE structure is fully cured using UV light, and the gel matrix can be washed away to generate a self-supporting structure as seen in Figure 2a. The primary variable affecting full curing of the LCE after embedded printing is the second-stage photocuring step initiated by the UV light. Further investigation of this can be found in Section S4 in the Supporting Information where Figure S4 demonstrates that the gel matrix depths used in this study did not affect the UV light dose; however, there may be limited curing of the LCE ink if gel depths increase above 50 mm. To generate self-supporting structures, the LCE ink must have good mechanical properties after removal from the gel. One way to achieve this is to add additional cross-links within the polymer chain. Pentaerythritol triacrylate (PETA) is a tetrafunctional acrylate ester that can be added to provide additional cross-linking sites during formation of the LCE ink. As seen in Figure 2b, PETA is critical for retaining the 3D shape of the printed LCE structures once they are removed from the gel. The resulting mechanical properties of printed LCE structures with varying concentrations of PETA were tested, as shown in Figure 2c.

https://doi.org/10.1021/acsami.3c14783
ACS Appl. Mater. Interfaces 2023, 15, 58897−58904

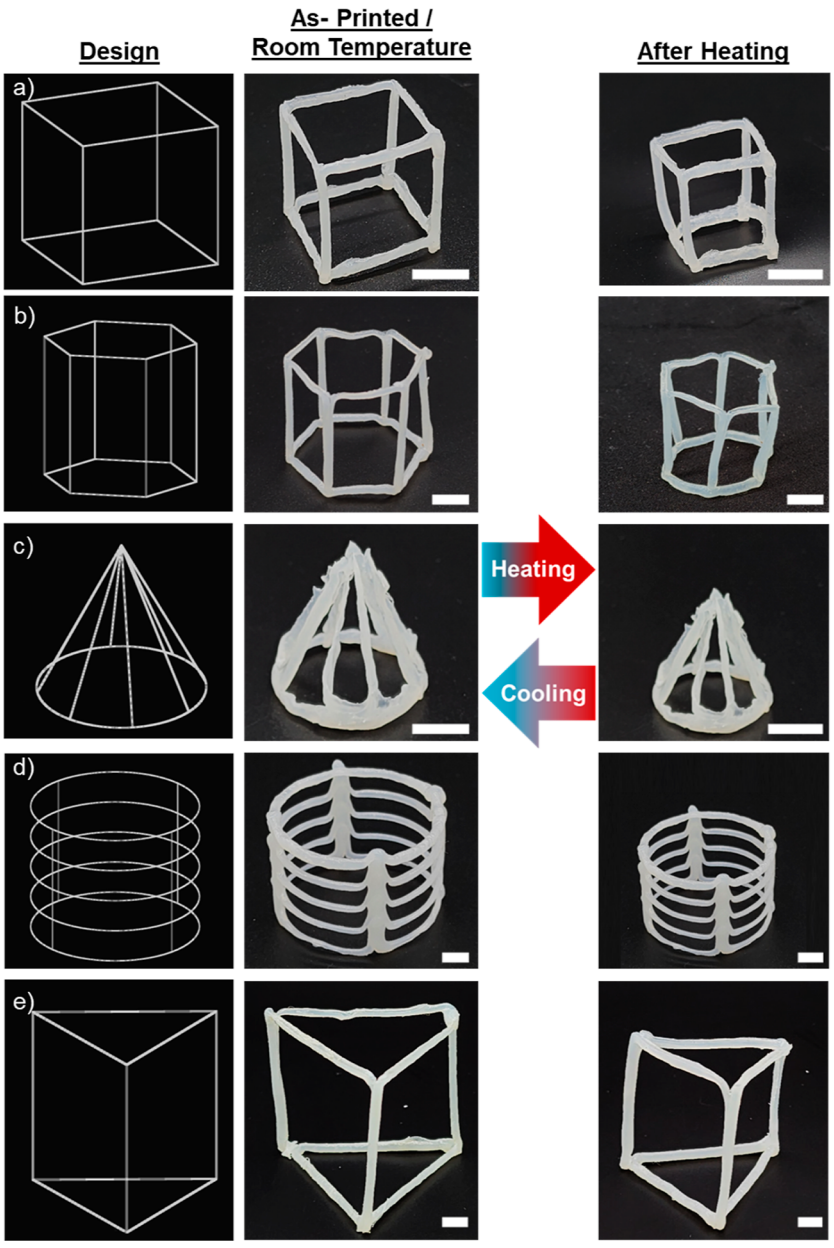

Figure 4. Embedded 4D printing of free-standing LCE structures that can achieve reversible shape transformations upon heating and cooling. (a) Cubic structure. (b) Hexagonal prism structure. (c) Conical structure. (d) Cylindrical ring structure. (e) Triangular prism structure. All scale bars are 5 mm.

When increasing the concentration of PETA, the modulus can increase from 1 to 7 MPa. Additionally, it was found that adding concentrations of PETA above 3 wt % resulted in a more brittle structure with no significant increase in modulus. The effect of PETA on the mechanical properties of printed LCE structures warrants further investigation in future studies.

2.3. Characterization of the LCE. After printing and removal from the gel matrix, the LCE mechanical actuation in response to the temperature was characterized. To provide a clear comparison between traditional printed LCE and embedded printing of LCEs, the same ink was printed under ambient conditions onto a glass slide. The influence of the LCE print direction on mechanical actuation was also studied. Figure 3a shows the thermomechanical response of LCE printed under ambient conditions onto a glass slide. These results match literature values for printed LCE in ambient conditions where print speed and corresponding mesogen alignment show a direct correlation with mechanical actuation strain.[54] When printed horizontally in the gel, the LCE exhibited a similar dependence on the print speed, as shown in Figure 3b. This indicates that embedded printing into a gel matrix has limited influence on LCE mesogen alignment. Furthermore, the maximum thermomechanical actuation strains of around 45% correspond with those observed in related studies where other mechanical alignment methods are used.[23,33] When printed vertically in the gel, the LCE thermomechanical actuation exhibited a similar dependence on the print speed. It can be noted, however, that at lower printing speeds the resulting mechanical actuation is limited. This may be attributed to differing mechanical boundary conditions during vertical extrusion of the LCE ink compared to horizontal extrusion. First, when printed horizontally, the

https://doi.org/10.1021/acsami.3c14783
ACS Appl. Mater. Interfaces 2023, 15, 58897−58904

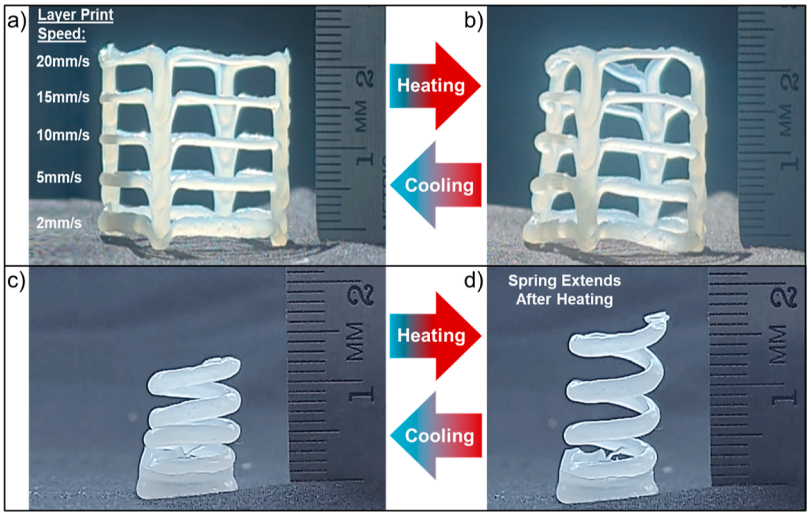

Figure 5. Demonstration of embedded 4D printing of LCE to achieve unique 3D shape transformations in response to temperature. (a) LCE ring structure with each layer printed using a different speed. (b) Actuation of the LCE ring structure showing that each ring actuates differently in response to heating. (c) LCE spring after printing and removal from gel matrix. (d) LCE spring exhibiting linear expansion in response to heating.

geometry of the printed LCE trace must change, resulting in mechanical shear forces that may increase the LCE mesogen alignment and actuation when compared to vertically printed LCE traces. Second, the boundary conditions of the printed trace are different when printed horizontally vs vertically. When printed horizontally, further mechanical stretching of the LCE mesogens may exist in previously printed portions of the LCE trace as the nozzle moves because it is constrained to the print or gel surface. Alternatively, when printed vertically, additional mechanical stretching of the LCE-printed trace during printing will likely not occur, especially at slow printing speeds. To investigate this, a comparison between the three printing conditions for three different printing speeds is plotted in Figure 3d–f. These results show that above a print speed of 5 mm/s, the influence of printing speed on the resulting thermomechanical actuation is similar for each of the three printing conditions. While the associated changes in mechanical actuation are small, around 8% for traces printed at 2 mm/s, further investigation of this effect should be considered in future studies. Lastly, the tensile mechanical properties of the LCE ink printed in ambient conditions vs in the gel were also studied and found to have nearly identical tensile properties. These results can be found in Section S5 in the Supporting Information.

2.4. 4D-Printed Free-Form LCE Structures. Generating free-standing LCE structures enables structures that can be functional in their initial state before deformation and transform to a secondary shape with new functionality. Here, we demonstrate free-form, freestanding 3D LCE geometries that can transform into new 3D shapes after heating. Figure 4a shows a cube architecture printed at 25 mm/s. As a result, when it is heated, homogeneous shrinkage strain of each of the printed lines results in a 50% shrinkage of the initial architecture. Upon cooling to room temperature, the cube returns to its initial configuration, representing a fully reversible shape transformation. More complex architectures could also be printed such as a hexagonal prism, as seen in Figure 4b. This structure can also shrink to 50% of its original size after heating and return to its initial shape after cooling to room temperature. Figure 4c shows a conical architecture. As seen, printing diagonally in the gel matrix can generate lines with a reduced resolution and some nonlinear actuation. Prior studies investigating the mechanics of embedded printing have shown that print resolution can be improved with further refinement of printing conditions such as print speed, gel matrix viscoelasticity, or ink rheology.[55] A cylindrical ring structure was printed, shown in Figure 4d, demonstrating that the gel provides support for long sections of a printed line. Lastly, a triangular prism was printed, as shown in Figure 4e, demonstrating a 100 mm tall structure. Like the previous demonstrations, the cylindrical ring structure and triangular prism structures were printed at 25 mm/s and could achieve reversible 50% shape changes upon heating and cooling. Further investigation into the resolution and size limitations of LCE printed lines will enable printing of increasingly complex architectures for specific applications. Additionally, further advances in 3D gcode generation techniques will enable further shape and design complexity.

2.5. Nonisotropic 3D Shape Transformations. Printing of free-form structures enables 3D to 3D shape transformations that have not yet been demonstrated using LCEs. Furthermore, by adjusting the LCE printing speed within the same structure, the variable mechanical actuations can be harnessed to generate tunable, nonisotropic shape transformations. Figure 5a shows a cylindrical ring structure where each ring is printed by using a different speed. By variation of the print speed, the resulting mechanical actuation can be modulated to generate a shape transformation from a cylindrical to a conical shape after heating, as seen in Figure 5b. This type of structure can be used for complex pick-and-place applications where variable gripping force is required. Figure 5c shows a printed LCE spring. Interestingly, when heated, the spring generates a linear expansion actuation of 33% (12–16 mm). As shown in Section 2.4, LCE generates up to 50% linear shrinkage strain in response to an increase in temperature. However, when printed into specific geometries, the shrinkage strain can be transformed to provide expansion strain. In this case, the uncoiling of the spring during heating can generate linear expansion. Videos of the structures actuating can be found in the Supporting Information. Many unique methods for regulating LCE mesogen alignment by modifying printing parameters have been explored in the literature[26,56,57] and can

https://doi.org/10.1021/acsami.3c14783
ACS Appl. Mater. Interfaces 2023, 15, 58897–58904

be implemented to generate further complexity during LCE actuation. Further 3D geometries should be explored to harness the unique shape transformation of LCE structures for more complex actuations such as snapping,[58] jumping,[59] or crawling.[5]

3. CONCLUSIONS

In this work, we report embedded 4D printing; a newly developed methodology for fabricating free-form, self-supporting 3D LCE structures which can generate unique shape transformations that have not previously been demonstrated in the literature. Embedded 4D printing of LCE into a laponite gel matrix provided a facile method for producing geometrically complex LCE structures. By increasing the cross-link density and resulting modulus of the LCE, the structures could retain their shape after removal from the gel. Furthermore, it was demonstrated that printing into the gel matrix has a limited effect on the thermomechanical actuation properties of LCE. The structures presented herein demonstrate significant advances in geometrical complexity over previously reported LCE architectures, ultimately resulting in unique 3D to 3D′ shape transformations. This work demonstrates a methodology for the preparation of geometrically complex smart structures that can be used for a variety of smart structure applications such as soft robotics, biomedical devices, and deployable structures.

4. MATERIALS AND METHODS

4.1. Materials. *4.1.1. Liquid Crystal Elastomer Ink.* The LCE ink used in this study was synthesized by following the procedure outlined below. First, RM257 and RM82, purchased from Wilshire Technologies (Princeton, NJ, USA), were mixed in a 75/25 weight ratio. Next, 25 wt % thiol spacer [2,2′-(ethylenedioxy) diethanethiol (EDDT)], 3 wt % of the tetrafunctional cross-linker [pentaerythritol triacrylate (PETA)], 5 wt % photoinitiator (Irgacure 651), and 2.5 wt % inhibitor (BHT) were introduced into the mixture. Each of these chemicals was obtained from Sigma-Aldrich (St. Louis, MO, USA). The solution was then heated to 100 °C and occasionally mixed to ensure homogeneity. After cooling to room temperature, 1 wt % catalyst [tetraethylamine (TEA) in a 1:20 ratio with toluene] was added. The solution was then added to a Thinky mixer (ARV 310, Thinky Inc., Laguna Hills, CA, USA) and stirred at 2000 rpm for 2 min. The solution was transferred to a 30 mL syringe and heated at 40 °C for 45 min for oligomerization. After removal from the oven and cooling to room temperature, the LCE ink was ready for printing.

4.1.2. Laponite Gel Matrix. The gel matrix was prepared using 4 wt % of laponite powder (Laponite-RD, BYK-Chemie GmbH, Wesel, Germany), with 96 wt % of distilled water. Laponite powder was evenly distributed into distilled water while being continuously stirred to ensure proper dispersion. After the laponite was added, the gel was allowed to sit for 24 h to allow for complete hydration and gel formation. After 24 h, the laponite gel is ready for use.

4.2. Printing and Characterization Methods. *4.2.1. Embedded Printing.* A custom-engineered direct ink write (DIW) system having computer-controlled motion stages was used to translate a built plate in the *X*−*Y* plane. A constant displacement syringe pump affixed to the translating motion stage of the *Z*-axis provided a method of depositing the LCE inks. The LCE inks were embedded in a 3D printed at room temperature into the laponite gel matrix.

4.2.2. Characterization of the Printed LCE. Characterization of the printed LCE structures was performed by using dynamic mechanical analysis (DMA 850, TA Instruments, New Castle, DE, USA). To test the mechanical actuation response of the LCE, samples were placed under a constant 0.1 N tensile load. The temperature was then ramped from 23 to 230 °C at a rate of 3°/min to measure the resulting mechanical actuation strain in response to temperature.

ASSOCIATED CONTENT

Supporting Information

The Supporting Information is available free of charge at https://pubs.acs.org/doi/10.1021/acsami.3c14783.

Further experiments and discussions (PDF)
Embedded 4D printing of free-form liquid crystal elastomer structure (MP4)
Actuation of the free-form LCE ring structure (MP4)
Linear expansion actuation of free-form LCE spring (MP4)

AUTHOR INFORMATION

Corresponding Authors

Bryan Kaehr − *Advanced Materials Laboratory, Sandia National Laboratories, Albuquerque, New Mexico 87106, United States;* orcid.org/0000-0002-9227-7060; Email: bkaehr@sandia.gov

Devin J. Roach − *Advanced Materials Laboratory, Sandia National Laboratories, Albuquerque, New Mexico 87106, United States; School of Mechanical, Industrial, and Manufacturing Engineering, Oregon State University, Corvallis, Oregon 97331, United States;* orcid.org/0000-0002-8825-0340; Email: devin.roach@oregonstate.edu

Authors

Luke McDougall − *Advanced Materials Laboratory, Sandia National Laboratories, Albuquerque, New Mexico 87106, United States*

Jeremy Herman − *Advanced Materials Laboratory, Sandia National Laboratories, Albuquerque, New Mexico 87106, United States; Department of Chemical and Biological Engineering, The University of Colorado, Boulder, Colorado 80309, United States*

Emily Huntley − *Advanced Materials Laboratory, Sandia National Laboratories, Albuquerque, New Mexico 87106, United States*

Samuel Leguizamon − *Advanced Materials Laboratory, Sandia National Laboratories, Albuquerque, New Mexico 87106, United States;* orcid.org/0000-0003-3395-6562

Adam Cook − *Advanced Materials Laboratory, Sandia National Laboratories, Albuquerque, New Mexico 87106, United States*

Timothy White − *Department of Chemical and Biological Engineering, The University of Colorado, Boulder, Colorado 80309, United States;* orcid.org/0000-0001-8006-7173

Complete contact information is available at: https://pubs.acs.org/10.1021/acsami.3c14783

Author Contributions

Conceptualization: D.J.R., B.K. Methodology: D.J.R., J.H., B.K. Investigation: L.M., D.J.R., J.H., E.H., S.L. Visualization: L.M., J.H., D.J.R. Supervision: D.J.R., T.W., B.K. Writing—original draft: D.J.R., L.M. Writing—review and editing: D.J.R., L.M., T.W., B.K.

Notes

The authors declare no competing financial interest.

ACKNOWLEDGMENTS

This work was performed, in part, at the Center for Integrated Nanotechnologies, an Office of Science User Facility operated for the U.S. Department of Energy (DOE) Office of Science. The Sandia National Laboratories is a multimission laboratory

managed and operated by the National Technology & Engineering Solutions of Sandia, LLC, a wholly owned subsidiary of Honeywell International, Inc., for the U.S. DOE's National Nuclear Security Administration under contract DE-NA-0003525. The views expressed in the article do not necessarily represent the views of the U.S. DOE or the United States Government. J.A.H. acknowledges support from the National Science Foundation via a Graduate Research Fellowship. T.J.W. acknowledges financial support from the Sandia National Laboratories and National Science Foundation DMR grant 2105369. The authors would like to thank Derek Reinholtz, Madison T. Hochrein, and Jorge Cardenas for their assistance with experimental operations.

REFERENCES

(1) Kuang, X.; Arıcan, M. O.; Zhou, T.; Zhao, X.; Zhang, Y. S. Functional Tough Hydrogels: Design, Processing, and Biomedical Applications. *Acc. Mater. Res.* **2023**, *4* (2), 101−114.
(2) Mohammadi, M.; Zolfagharian, A.; Bodaghi, M.; Xiang, Y.; Kouzani, A. Z. 4D printing of soft orthoses for tremor suppression. *Bio-Des. Manuf.* **2022**, *5* (4), 786−807.
(3) Afzali Naniz, M.; Askari, M.; Zolfagharian, A.; Afzali Naniz, M.; Bodaghi, M. 4D printing: a cutting-edge platform for biomedical applications. *Biomed. Mater.* **2022**, *17* (6), 062001.
(4) Wang, Y.; Cui, H.; Esworthy, T.; Mei, D.; Wang, Y.; Zhang, L. G. Emerging 4D Printing Strategies for Next-Generation Tissue Regeneration and Medical Devices. *Adv. Mater.* **2022**, *34* (20), 2109198.
(5) He, Q.; Yin, R.; Hua, Y.; Jiao, W.; Mo, C.; Shu, H.; Raney, J. R. A modular strategy for distributed, embodied control of electronics-free soft robots. *Sci. Adv.* **2023**, *9* (27), No. eade9247.
(6) Kim, Y.; Yuk, H.; Zhao, R.; Chester, S. A.; Zhao, X. Printing ferromagnetic domains for untethered fast-transforming soft materials. *Nature* **2018**, *558* (7709), 274−279.
(7) Roach, D. J.; Sun, X.; Peng, X.; Demoly, F.; Zhou, K.; Qi, H. J. 4D Printed Multifunctional Composites with Cooling-Rate Mediated Tunable Shape Morphing. *Adv. Funct. Mater.* **2022**, *32* (36), 2203236.
(8) Zolfagharian, A.; Kaynak, A.; Kouzani, A. Closed-loop 4D-printed soft robots. *Mater. Des.* **2020**, *188*, 108411.
(9) Ware, T. H.; McConney, M. E.; Wie, J. J.; Tondiglia, V. P.; White, T. J. Voxelated liquid crystal elastomers. *Science* **2015**, *347* (6225), 982−984.
(10) Vinciguerra, M. R.; Patel, D. K.; Zu, W.; Tavakoli, M.; Majidi, C.; Yao, L. Multimaterial Printing of Liquid Crystal Elastomers with Integrated Stretchable Electronics. *ACS Appl. Mater. Interfaces* **2023**, *15* (20), 24777−24787.
(11) Kaufman, G.; Jimenez, J.; Bradshaw, A.; Radecka, A.; Gallegos, M.; Kaehr, B.; Golecki, H. A Stiff-Soft Composite Fabrication Strategy for Fiber Optic Tethered Microtools. *Adv. Mater. Technol.* **2023**, *8* (12), 2202034.
(12) Wu, S.; Eichenberger, J.; Dai, J.; Chang, Y.; Ghalichechian, N.; Zhao, R. R. Magnetically Actuated Reconfigurable Metamaterials as Conformal Electromagnetic Filters. *Advanced Intelligent Systems* **2022**, *4* (9), 2200106.
(13) He, Q.; Zheng, Y.; Wang, Z.; He, X.; Cai, S. Anomalous inflation of a nematic balloon. *J. Mech. Phys. Solid.* **2020**, *142*, 104013.
(14) Tibbits, S. 4D Printing: Multi-Material Shape Change. *Architect. Des* **2014**, *84* (1), 116−121.
(15) Wang, Z.; Li, K.; He, Q.; Cai, S. A Light-Powered Ultralight Tensegrity Robot with High Deformability and Load Capacity. *Adv. Mater.* **2019**, *31* (7), 1806849.
(16) Martinez, A. M.; McBride, M. K.; White, T. J.; Bowman, C. N. Reconfigurable and Spatially Programmable Chameleon Skin-Like Material Utilizing Light Responsive Covalent Adaptable Cholesteric Liquid Crystal Elastomers. *Adv. Funct. Mater.* **2020**, *30* (35), 2003150.
(17) Montesino, L.; Martínez, J. I.; Sánchez-Somolinos, C. Reprogrammable 4D Printed Liquid Crystal Elastomer Photo-actuators by Means of Light-Reversible Perylene Diimide Radicals. *Adv. Funct. Mater.* **2023**, *n/a* (n/a), 2309019.
(18) He, Q.; Wang, Z.; Song, Z.; Cai, S. Bioinspired Design of Vascular Artificial Muscle. *Adv. Mater. Technol.* **2019**, *4* (1), 1800244.
(19) Roach, D. J.; Yuan, C.; Kuang, X.; Li, V. C.-F.; Blake, P.; Romero, M. L.; Hammel, I.; Yu, K.; Qi, H. J. Long Liquid Crystal Elastomer Fibers with Large Reversible Actuation Strains for Smart Textiles and Artificial Muscles. *ACS Appl. Mater. Interfaces* **2019**, *11* (21), 19514−19521.
(20) Zhang, J.; Guo, Y.; Hu, W.; Soon, R. H.; Davidson, Z. S.; Sitti, M. Liquid Crystal Elastomer-Based Magnetic Composite Films for Reconfigurable Shape-Morphing Soft Miniature Machines. *Adv. Mater.* **2021**, *33* (8), 2006191.
(21) Chen, S.-H.; Amer, N. M. Observation of Macroscopic Collective Behavior and New Texture in Magnetically Doped Liquid Crystals. *Phys. Rev. Lett.* **1983**, *51* (25), 2298−2301.
(22) Velasco Abadia, A.; Bauman, G. E.; White, T. J.; Schwartz, D. K.; Kaar, J. L. Direct Ink Writing of Enzyme-Containing Liquid Crystal Elastomers as Versatile Biomolecular-Responsive Actuators. *Adv. Mater. Interfaces* **2023**, *10* (22), 2300086.
(23) Yakacki, C. M.; Saed, M.; Nair, D. P.; Gong, T.; Reed, S. M.; Bowman, C. N. Tailorable and programmable liquid-crystalline elastomers using a two-stage thiol−acrylate reaction. *RSC Adv.* **2015**, *5* (25), 18997−19001.
(24) Lugger, S. J. D.; Engels, T. A. P.; Cardinaels, R.; Bus, T.; Mulder, D. J.; Schenning, A. P. H. J. Melt-Extruded Thermoplastic Liquid Crystal Elastomer Rotating Fiber Actuators. *Adv. Funct. Mater.* **2023**, *33* (49), 2306853.
(25) Shin, J.; Kang, M.; Tsai, T.; Leal, C.; Braun, P. V.; Cahill, D. G. Thermally Functional Liquid Crystal Networks by Magnetic Field Driven Molecular Orientation. *ACS Macro Lett.* **2016**, *5* (8), 955−960.
(26) Wang, Z.; Wang, Z.; Zheng, Y.; He, Q.; Wang, Y.; Cai, S. Three-dimensional printing of functionally graded liquid crystal elastomer. *Sci. Adv.* **2020**, *6* (39), No. eabc0034.
(27) Javadzadeh, M.; del Barrio, J.; Sánchez-Somolinos, C. Melt Electrowriting of Liquid Crystal Elastomer Scaffolds with Programmed Mechanical Response. *Adv. Mater.* **2023**, *35* (14), 2209244.
(28) Saed, M. O.; Ambulo, C. P.; Kim, H.; De, R.; Raval, V.; Searles, K.; Siddiqui, D. A.; Cue, J. M. O.; Stefan, M. C.; Shankar, M. R.; Ware, T. H. Molecularly-Engineered, 4D-Printed Liquid Crystal Elastomer Actuators. *Adv. Funct. Mater.* **2019**, *29* (3), 1806412.
(29) Peng, X.; Wu, S.; Sun, X.; Yue, L.; Montgomery, S. M.; Demoly, F.; Zhou, K.; Zhao, R. R.; Qi, H. J. 4D Printing of Freestanding Liquid Crystal Elastomers via Hybrid Additive Manufacturing. *Adv. Mater.* **2022**, *34* (39), 2204890.
(30) Yue, L.; Sun, X.; Yu, L.; Li, M.; Montgomery, S. M.; Song, Y.; Nomura, T.; Tanaka, M.; Qi, H. J. Cold-programmed shape-morphing structures based on grayscale digital light processing 4D printing. *Nat. Commun.* **2023**, *14* (1), 5519.
(31) Jin, B.; Liu, J.; Shi, Y.; Chen, G.; Zhao, Q.; Yang, S. Solvent-Assisted 4D Programming and Reprogramming of Liquid Crystalline Organogels. *Adv. Mater.* **2022**, *34* (5), 2107855.
(32) Chen, G.; Jin, B.; Shi, Y.; Zhao, Q.; Shen, Y.; Xie, T. Rapidly and Repeatedly Reprogrammable Liquid Crystalline Elastomer via a Shape Memory Mechanism. *Adv. Mater.* **2022**, *34* (21), 2201679.
(33) Tabrizi, M.; Ware, T. H.; Shankar, M. R. Voxelated Molecular Patterning in Three-Dimensional Freeforms. *ACS Appl. Mater. Interfaces* **2019**, *11* (31), 28236−28245.
(34) Li, S.; Bai, H.; Liu, Z.; Zhang, X.; Huang, C.; Wiesner, L. W.; Silberstein, M.; Shepherd, R. F. Digital light processing of liquid crystal elastomers for self-sensing artificial muscles. *Sci. Adv.* **2021**, *7* (30), No. eabg3677.
(35) Zarzar, L. D.; Kim, P.; Kolle, M.; Brinker, C. J.; Aizenberg, J.; Kaehr, B. Direct Writing and Actuation of Three-Dimensionally Patterned Hydrogel Pads on Micropillar Supports. *Angew. Chem., Int. Ed.* **2011**, *50* (40), 9356−9360.

(36) Kaehr, B.; Shear, J. B. Multiphoton fabrication of chemically responsive protein hydrogels for microactuation. *Proc. Natl. Acad. Sci. U.S.A.* **2008**, *105* (26), 8850−8854.
(37) Münchinger, A.; Hahn, V.; Beutel, D.; Woska, S.; Monti, J.; Rockstuhl, C.; Blasco, E.; Wegener, M. Multi-Photon 4D Printing of Complex Liquid Crystalline Microstructures by In Situ Alignment Using Electric Fields. *Adv. Mater. Technol.* **2021**, *n/a* (n/a), 2100944.
(38) Zeng, H.; Wasylczyk, P.; Parmeggiani, C.; Martella, D.; Burresi, M.; Wiersma, D. S. Light-Fueled Microscopic Walkers. *Adv. Mater.* **2015**, *27* (26), 3883−3887.
(39) del Pozo, M.; Delaney, C.; Pilz da Cunha, M.; Debije, M. G.; Florea, L.; Schenning, A. P. H. J. Temperature-Responsive 4D Liquid Crystal Microactuators Fabricated by Direct Laser Writing by Two-Photon Polymerization. *Small Struct.* **2022**, *3* (2), 2100158.
(40) Weeks, R. D.; Truby, R. L.; Uzel, S. G. M.; Lewis, J. A. Embedded 3D Printing of Multimaterial Polymer Lattices via Graph-Based Print Path Planning. *Adv. Mater.* **2023**, *35* (5), 2206958.
(41) Hajash, K.; Sparrman, B.; Guberan, C.; Laucks, J.; Tibbits, S. Large-Scale Rapid Liquid Printing. *3D Printing and Additive Manufacturing* **2017**, *4* (3), 123−132.
(42) Kajtez, J.; Wesseler, M. F.; Birtele, M.; Khorasgani, F. R.; Rylander Ottosson, D.; Heiskanen, A.; Kamperman, T.; Leijten, J.; Martínez-Serrano, A.; Larsen, N. B.; Angelini, T. E.; Parmar, M.; Lind, J. U.; Emnéus, J. Embedded 3D Printing in Self-Healing Annealable Composites for Precise Patterning of Functionally Mature Human Neural Constructs. *Advanced Science* **2022**, *9* (25), 2201392.
(43) Zeng, X.; Meng, Z.; He, J.; Mao, M.; Li, X.; Chen, P.; Fan, J.; Li, D. Embedded bioprinting for designer 3D tissue constructs with complex structural organization. *Acta Biomater.* **2022**, *140*, 1−22.
(44) Wu, W.; DeConinck, A.; Lewis, J. A. Omnidirectional Printing of 3D Microvascular Networks. *Adv. Mater.* **2011**, *23* (24), H178−H183.
(45) Gao, K.; Gong, J.; Cao, P.; Tang, Z.; Wang, T.; Tao, L.; Zhang, X.; Zhang, J.; Wang, Q.; Zhang, Y. Toward 4D Printing of Shape Memory Polymers Based on Polyaryletherketone/NVP/PEGDA through Molecular Engineering and Direct Ink Writing 3D Printing. *ACS Appl. Polym. Mater.* **2023**, *5* (11), 8833−8844.
(46) Luo, K.; Wang, L.; Wang, M.-X.; Du, R.; Tang, L.; Yang, K.-K.; Wang, Y.-Z. 4D Printing of Biocompatible Scaffolds via In Situ Photo-crosslinking from Shape Memory Copolyesters. *ACS Appl. Mater. Interfaces* **2023**, *15* (37), 44373−44383.
(47) Basu, A.; Saha, A.; Goodman, C.; Shafranek, R. T.; Nelson, A. Catalytically Initiated Gel-in-Gel Printing of Composite Hydrogels. *ACS Appl. Mater. Interfaces* **2017**, *9* (46), 40898−40904.
(48) Uchida, T.; Onoe, H. 4D Printing of Multi-Hydrogels Using Direct Ink Writing in a Supporting Viscous Liquid. *Micromachines* **2019**, *10*, 433.
(49) Sydney Gladman, A.; Matsumoto, E. A.; Nuzzo, R. G.; Mahadevan, L.; Lewis, J. A. Biomimetic 4D printing. *Nat. Mater.* **2016**, *15* (4), 413−418.
(50) Jiang, Y.; Dong, X.; Wang, Q.; Dai, S.; Li, L.; Yuan, N.; Ding, J. A High-Fidelity Preparation Method for Liquid Crystal Elastomer Actuators. *Langmuir* **2022**, *38* (23), 7190−7197.
(51) Barnes, M.; Sajadi, S. M.; Parekh, S.; Rahman, M. M.; Ajayan, P. M.; Verduzco, R. Reactive 3D Printing of Shape-Programmable Liquid Crystal Elastomer Actuators. *ACS Appl. Mater. Interfaces* **2020**, *12* (25), 28692−28699.
(52) Roach, D. J.; Kuang, X.; Yuan, C.; Chen, K.; Qi, H. J. Novel ink for ambient condition printing of liquid crystal elastomers for 4D printing. *Smart Mater. Struct.* **2018**, *27* (12), 125011.
(53) Mahmoudi, M.; Burlison, S. R.; Moreno, S.; Minary-Jolandan, M. Additive-Free and Support-Free 3D Printing of Thermosetting Polymers with Isotropic Mechanical Properties. *ACS Appl. Mater. Interfaces* **2021**, *13* (4), 5529−5538.
(54) Bauman, G. E.; Hoang, J. D.; Toney, M. F.; White, T. J. Degree of Orientation in Liquid Crystalline Elastomers Defines the Magnitude and Rate of Actuation. *ACS Macro Lett.* **2023**, *12* (2), 248−254.
(55) O'Bryan, C. S.; Bhattacharjee, T.; Hart, S.; Kabb, C. P.; Schulze, K. D.; Chilakala, I.; Sumerlin, B. S.; Sawyer, W. G.; Angelini, T. E. Self-assembled micro-organogels for 3D printing silicone structures. *Sci. Adv.* **2017**, *3* (5), No. e1602800.
(56) Ren, L.; He, Y.; Ren, L.; Wang, Z.; Zhou, X.; Wu, Q.; Wang, K.; Li, B.; Liu, Q. Multi-parameter-encoded 4D printing of liquid crystal elastomers for programmable shape morphing behaviors. *Addit. Manuf.* **2023**, *61*, 103376.
(57) Wang, Z.; Boechler, N.; Cai, S. Anisotropic mechanical behavior of 3D printed liquid crystal elastomer. *Addit. Manuf.* **2022**, *52*, 102678.
(58) Hebner, T. S.; Korner, K.; Bowman, C. N.; Bhattacharya, K.; White, T. J. Leaping liquid crystal elastomers. *Sci. Adv.* **2023**, *9* (3), No. eade1320.
(59) Tsai, S.; Wang, Q.; Wang, Y.; King, W. P.; Tawfick, S. Miniature soft jumping robots made by additive manufacturing. *Smart Mater. Struct.* **2023**, *32* (10), 105022.

https://doi.org/10.1021/acsami.3c14783
ACS Appl. Mater. Interfaces 2023, 15, 58897−58904